ORIGINAL PAPER

Failure mechanism of a destructive landslide in Hosein Abad Kalpush Village, Semnan, Iran

Ali Lashgari[1,2] · Abdolhosein Haddad[1]

Abstract

A destructive landslide occurred in spring 2019, in Hosein Abad Kalpush Village, Northeast of Iran, after an unusually rainy period. Significant damages were observed in buildings and roads located on the slope failure zone. This paper represents a preliminary reconnaissance report prepared through the site visit done by the authors, a few days following the landslide occurrence. Then, the geotechnical and geophysical properties of the sliding area are reported using the site investigation tests. Subsequently, the rainfall data are incorporated for numerical slope stability analyses. This study shows the variation of the failure mechanism of the slope before and after rainfall. The results confirm that the factor of safety decreases 1.78 times after a 3-month period of rain with rainfall intensity about 6 times the long-term average. Finally, the performance of two slope stability improvement strategies is evaluated to mitigate the landslide hazard. The results of the study can provide a perspective on the climate change impacts in Iran for future geosystem designs, geohazard prediction, and the selection of rainfall-induced landslide mitigation strategies.

Notation

CL	Clay layer
RQD	Rock quality designation
V_s	Shear wave velocity
LL	Liquid limit
PI	Plasticity index
γ_{wet}	Wet unit weight
γ_{sat}	Saturated unit weight
G_s	Specific gravity of soil
C'	Soil cohesion
ϕ'	Soil friction angle
K	Permeability coefficient
FS	Factors of safety
I	Rainfall intensity threshold for landslide triggering
D	Rainfall duration
Disp.	Displacement
E	Elastic modulus
v	Poisson's ratio

✉ Abdolhosein Haddad
  haddad@semnan.ac.ir

  Ali Lashgari
  ali.lashgarii@alum.semnan.ac.ir

[1] Department of Civil Engineering, Semnan University, Semnan, Iran

[2] International Institute of Earthquake Engineering and Seismology, Tehran, Iran

Introduction

Climate change can considerably affect the intensity, frequency, and duration of extreme precipitation events (USGCRP 2009; IPCC 2013). The variations of precipitation characteristics can lead the behavior of a slope toward instability conditions. In recent years, many landslides have been reported worldwide and heavy precipitation was the main cause of failure. For example, a rain-induced landslide occurred in Aranayaka, Sri Lanka, in 2016 killing 127 people and destroying 75 houses (Dang et al. 2019). In March 2019, a 40-m wide landslide with an approximate volume of 35,000 m³ displaced and ruptured a gas pipeline after heavy rain in Taleghan County, Iran, resulting in the suspension of gas supply to more than 12,000 users (Vasseghi et al. 2021). Accordingly, the combination of an unusually rainy period and a landslide can lead to a costly disaster when the failure/triggering mechanism is not appropriately predicted.
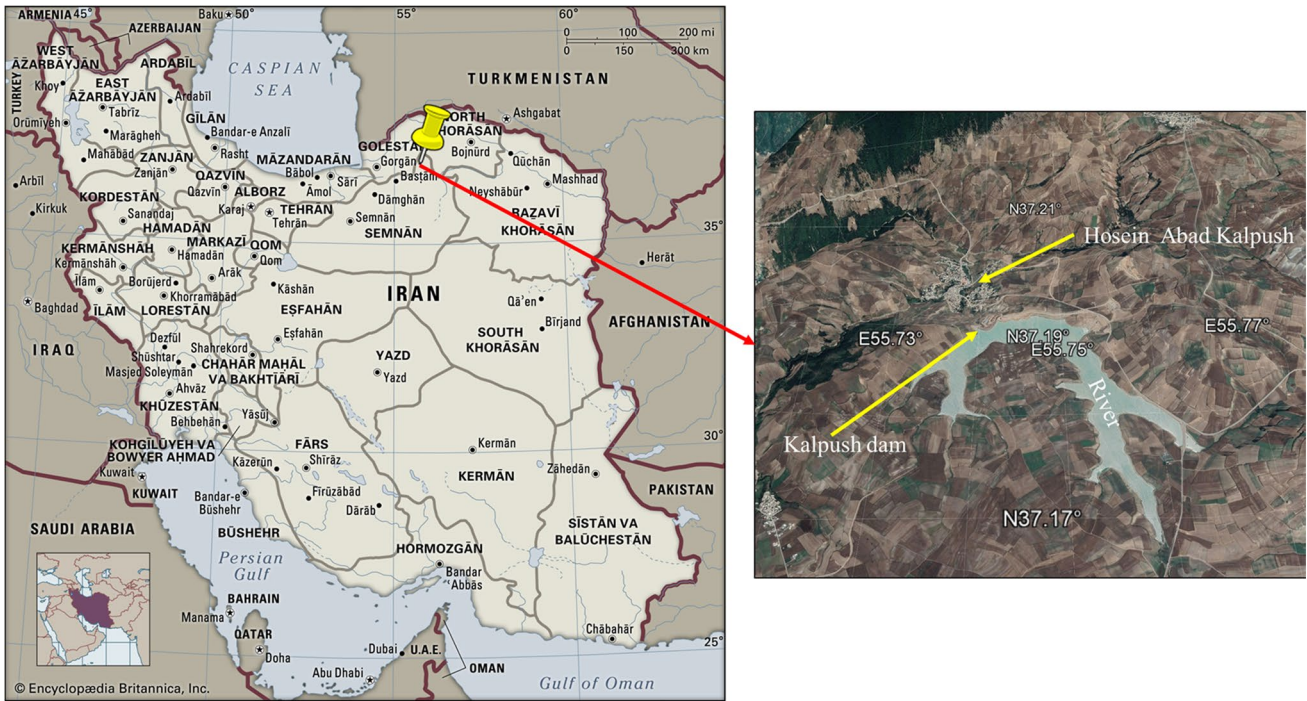
Fig. 1 Location map of the Kalpush dam and Hosein Abad Kalpush Village

Failure mechanisms of rainfall-induced landslides have recently been investigated by researchers to achieve a suitable prediction of slope failure behavior (e.g., Chien-Yuan et al. 2005; Zhang et al. 2022). Different approaches were generally employed in this field including (1) analytical methods (e.g., Di et al. 2021), (2) semi-empirical models
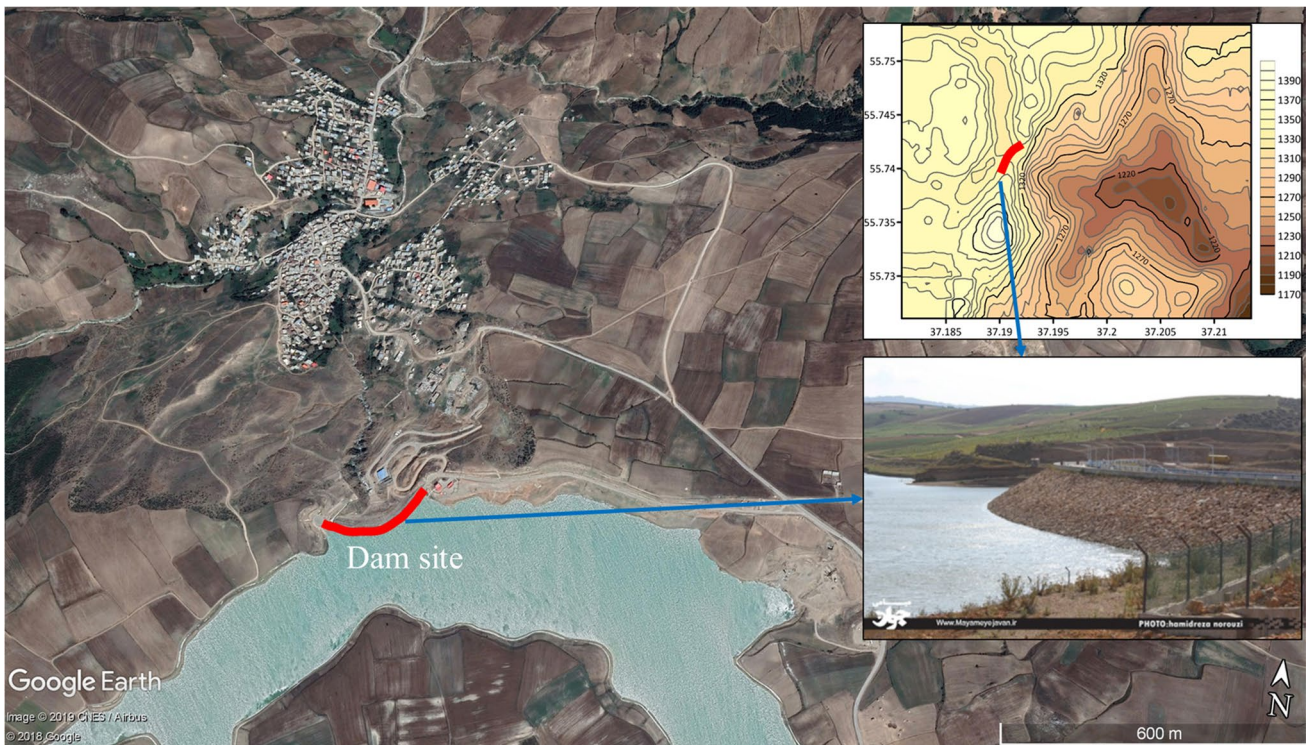

Fig. 2 Dam position and topography contour lines of the study area

that present the rainfall threshold for the initiation of the landslide (e.g., Guzzetti et al. 2008), (3) physical modeling (e.g., Askarinejad, et al. 2012; Li et al. 2016), and (4) numerical (e.g., Rivera-Hernandez et al. 2019; Paswan and Shrivastava 2022). The analytical methods are based on the determination of slope safety factor using an analytical solution and cuspidation of the variation of soil shear strength due to matric suction. The calculation of semi-empirical models is based on the statistical analysis of individual or multiple rainfall events that resulted in landslides in the past to define a threshold model (e.g., Caine 1980; Dahal and Hasegawa 2008). However, it is tough to analyze the actual mechanism of a rainfall-induced landslide only using the analytical methods and semi-empirical models because of the unpredictable nature of rainfall-induced landslides (e.g., Li et al. 2016). The numerical analyses can appropriately simulate the failure mechanism of slope since the interaction between the solid and fluid is considered by these analyses as an important factor in rainfall-induced landslide modeling (e.g., Zhao et al. 2017; Vahedifard et al. 2017). However, the numerical analysis of a rainfall sliding needs a case study for verification of the model and the lack of appropriate case studies and input parameters can affect the accuracy of the numerical models. Accordingly, a case study of rainfall-induced landslides can provide a suitable comprehension of the interaction between sliding failure mechanisms, rainfall intensity, and structural damages for practicing engineers. Moreover, the selection of suitable ground improvement techniques for the mitigation of landslide hazards depends on the landslide triggering factors besides site properties and project requirements (e.g., Alimohammadi et al. 2022).

Climate change can have a different impact on the rainfall patterns (e.g., amount of rainfall or rainfall duration) in different parts of the world (Loo et al. 2015). Many studies demonstrated that the failure mechanism of a slope can be different subject to a local rainfall pattern. The numerical stability analysis by Kristo et al. (2017) showed that the factor of safety significantly decreases from 2003 to 2050 due to an increase in rainfall intensity in Singapore. Vaghefi et al. (2019) showed that Iran will experience a climate of extended dry periods interrupted by intermittent heavy rainfalls in the future. Moreover, Iran is subjected to diffuse phenomena of landslide, due to its topographic and geological characteristics (e.g., Alborz Mountain in the north and Zagros Mountain in the west). Accordingly, the evaluation of the failure mechanism of rainfall-induced landslides can provide a perspective on the climate change impacts in Iran for future geosystem designs, geohazard prediction, and landslide mitigation strategies. However, a few studies (e.g., Alimohammadlou et al. 2014) have focused on the numerical simulation of slope performance during rainfall by providing the details of a case history.

In this study, the characteristics and failure mechanisms of the landslide are investigated during rainfall. First, the characteristics of the landslide and the structural and geotechnical damages are presented by the field surveys. Second, the geotechnical and geophysical properties of the sliding area are estimated using the site investigation tests. Third, the rainfall data are presented and discussed the possible causes of the landslide. Subsequently, a series of numerical simulations were carried out to comprehend the failure mechanism of the landslide for three sections of slope using the safety factor and deformation analyses. Furthermore, the results are compared to the observed damages. Finally, the performance of two landslide mitigation techniques is analyzed and compared to improve slope stability.

Study area

The Kalpush landslide occurred in Kalpush Village, Meyami County, Semnan Province, Northeast of Iran at coordinates of N 37° 11′ 42″ and E 55° 44′ 29″, where the Kalpush dam, which is an earth dam, was constructed near it on Hosein Abad river in 2013. The height of the dam from the foundation, the length of the crest of the dam, and the normal capacity of the dam are 43 m, 273 m, and 16.7 Mm³, respectively. The normal water height of the dam reservoir is around 41 m. This dam supports agriculture. The deposits of the Hosein Abad Village and the Kalpush dam are shown in Fig. 1.

The residents of Hosein Abad Village reported several slow-moving landslides after the construction of the earth dam. Moreover, water seepage was reported from the dam reservoir/rivers in downstream of the dam in February 2019. The first significant landslide was observed in February and March 2019 after heavy rainfall in this area. During the first landslide, about 120 houses were damaged, and about 50 houses tolerated near the collapse level. The site visit of the authors in June 2019 indicated that the damaged houses increase to about 570 that about 250 houses experienced collapse or near-collapse levels. Accordingly, the Kalpush landslide provides a unique opportunity to study the failure mechanism of the slope after heavy rainfall and landslide damage at the urban area scale.

The study area has a lot of climatic variety since it was located on the border of the Semnan and Golestan provinces. These provinces have very diverse climatic conditions. The climate of Semnan Province has relatively a hot desert climate, while the Golestan Province has a mild and humid climate due to being close to the Caspian Sea. The average annual temperature and rainfall of the study area are about 1.1°C and 440 mm, respectively, so that 50% of the total annual rainfall occurs in January, February, and March. The topography contour lines of the study area are

shown in Fig. 2. As shown in Fig. 2, its topography includes mountains and valleys so that the elevation of the dam crest decreases from 1343 to 1213 m on the valley floor within 972 m. Accordingly, the topographic variation has increased the potential of landslide occurrence in this area (e.g., Jafarian and Lashgari 2017a; Lashgari et al. 2018). It is noted that the seismic hazard level is very high in this area based on the seismic standard of Iran (BHRC 2014). Accordingly, an earthquake can also lead to a larger displacement during the sliding (e.g., Jafarian et al. (2019); Lashgari et al. 2020; Javdanian and Pradhan 2019; Lashgari et al. 2021; Javdanian et al. 2022).

Characteristics of the landslide

The landslide zone is shown in Fig. 3. The field surveys indicate that the characteristics of the Kalpush landslide correspond to the behavior of a translational landslide (Highland and Bobrowsky 2008). As shown in Fig. 3(a), the area and volume of sliding mass are 146,000m^2 and 1,071,640m^3, respectively. Moreover, the sliding length is around 684 m, while its maximum width is about 339 m. The crown of the landslide started from the left wing of the dam in the downward stream, as shown in Fig. 3(a). The distance between the crown of the landslide and the upstream water level is about 166 m. The toe of the landslide was located in the down of the valley. The elevation of the crown and toe is 1349 m and 1234 m, respectively. It is noted that water flow was observed at the toe of the landslide during the field survey. Figure 3b shows

Fig. 3 Location of the landslide. **a** 2019 and **b** 2010
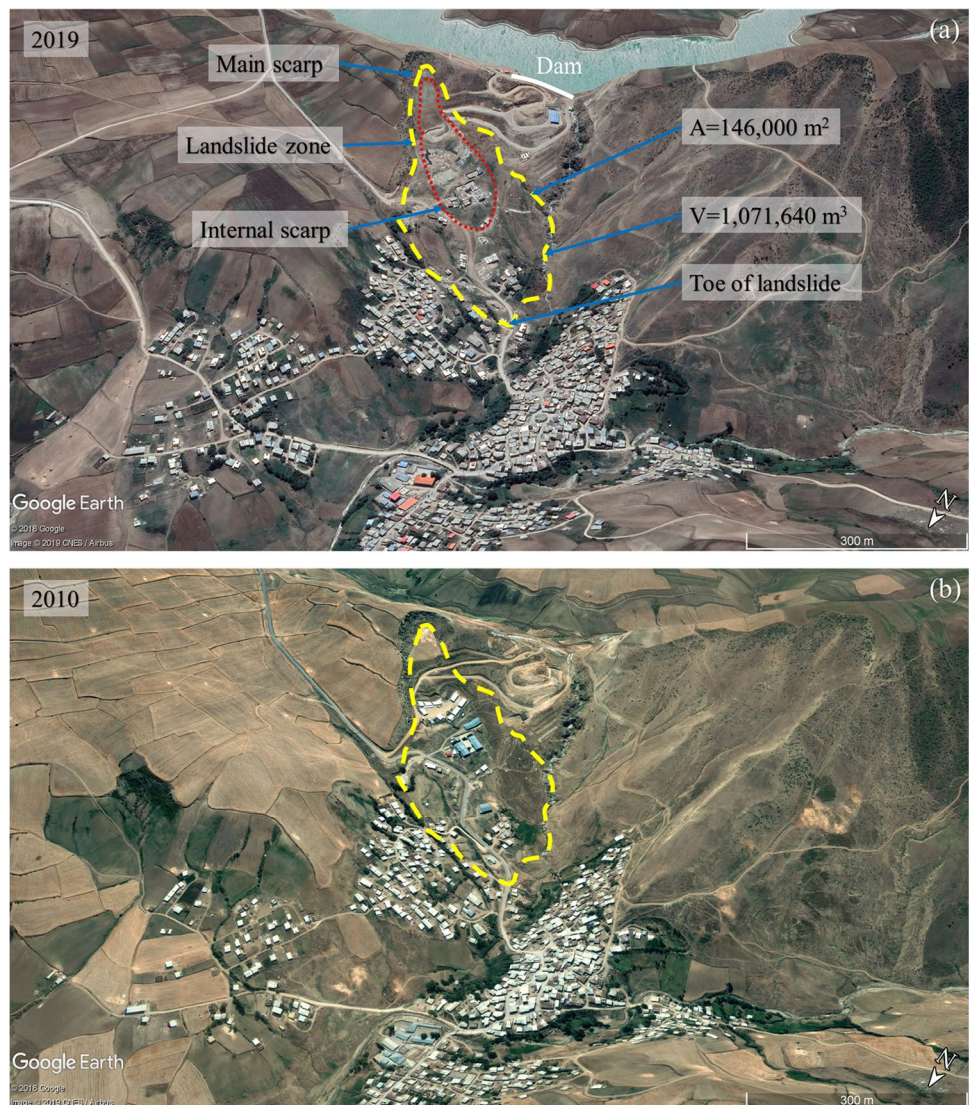
the properties of the landslide area in 2010. Comparison between Fig. 3 a and b shows the variations of the ground surface between 2010 and 2019.

The sliding direction is shown in Fig. 4(a). The sliding mass has gradually moved downward from January 2019 to March 2019. The average slope angle is around 8.93°, while the maximum slope angle is around 17.23°. The maximum displacement was observed at the head of the sliding area where the access road of the dam moved around 20–25 m. The cross section along line A-A is plotted in Fig. 4(b).
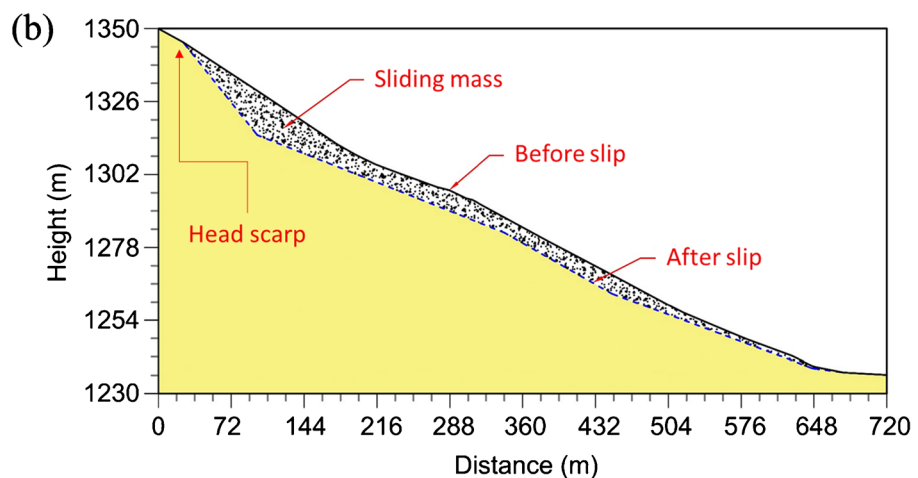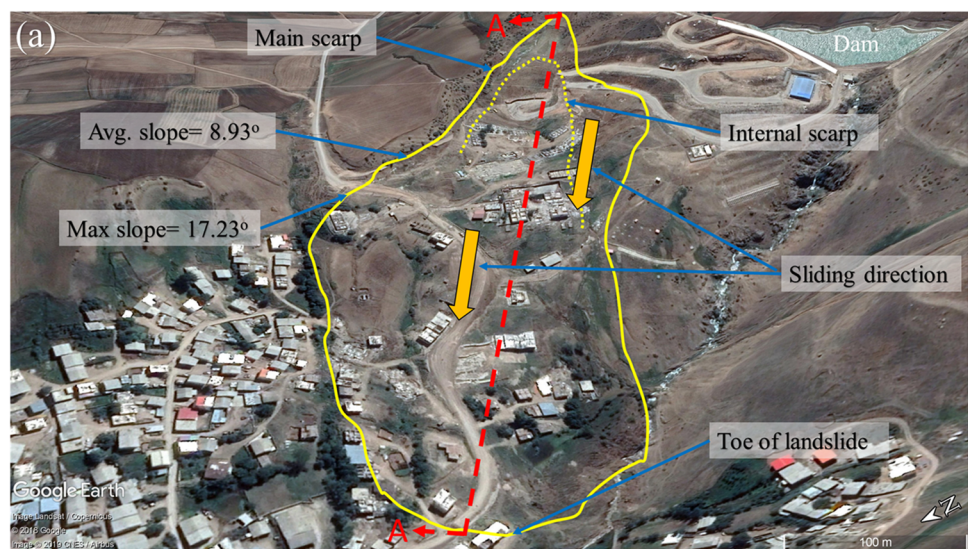
Landslide damages

Field investigation in May 2019 indicated that different damages occurred during this landslide. The access roads of the dam and village and the structures located on the sliding surface have experienced large displacements. The scattering of damages is shown in Fig. 5. As seen in Fig. 5, the structures

located on the center axis of sliding tolerated a large deformation at near-collapse and collapse levels. The building damage level is classified based on the deformations of the building elements. Palmisano et al. (2018) proposed a damage classification for masonry and reinforced concrete buildings. According to Palmisano et al. (2018), buildings with crack width of more than 5 mm in masonry elements and more than 4 mm in reinforced concrete beams and floors are categorized into the damage level of near collapse and collapse, respectively. Generally, more than 200 houses experienced collapse or are near-collapse levels. Moreover, the dam access road was destroyed and a new road has been established to access the dam.

Figure 6 shows the different landslide-induced damages. Figure 6a and c indicate that the movement of sliding mass significantly affects the structures built on the main body of the landslide. Figure 6c demonstrates a school that was destroyed due to the large displacement of sliding mass. Figure 6b shows a masonry structure located on the eastern border of the landslide that has moved downstream of the dam.

Fig. 4 a Characteristics of the landslide and **b** cross section of slope
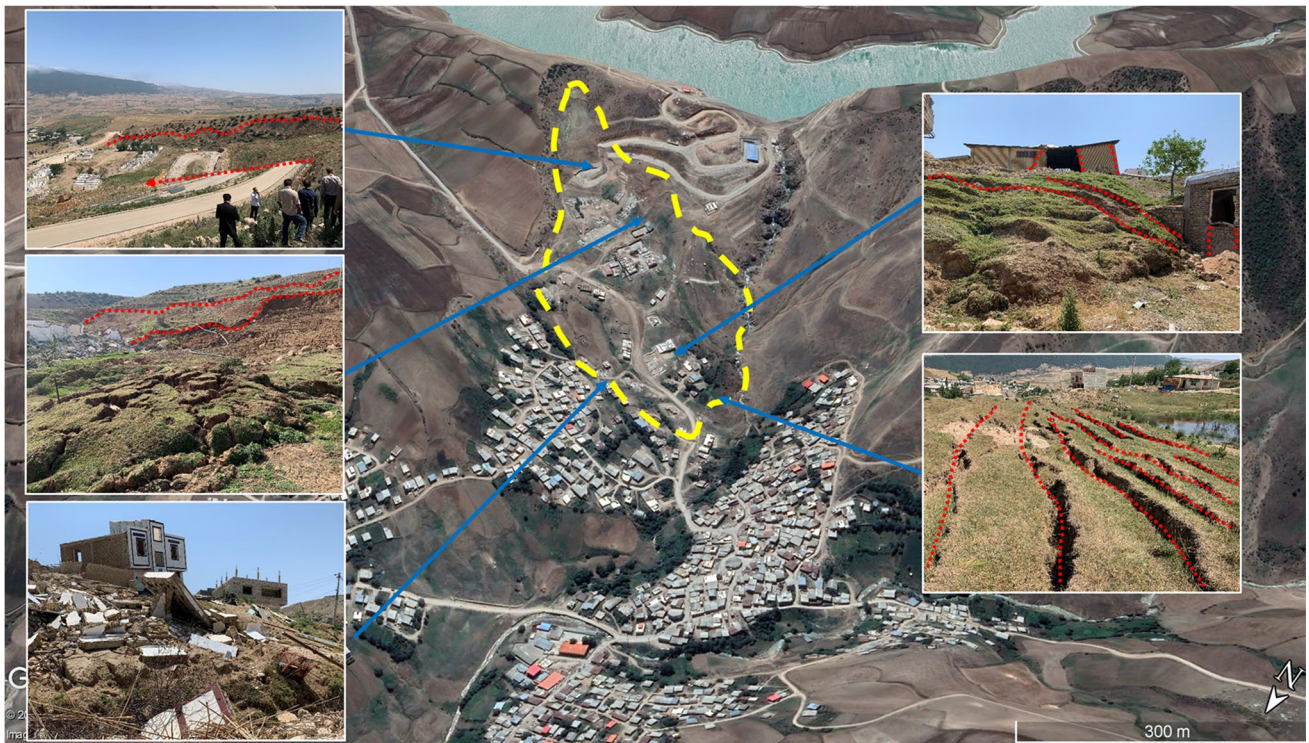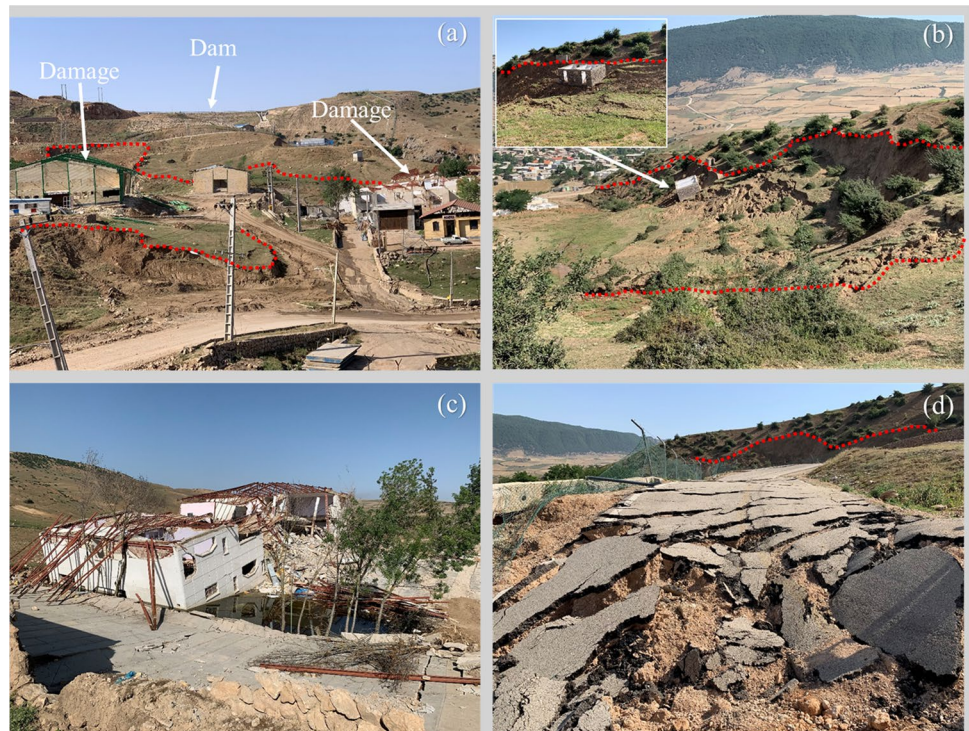
Fig. 5 Distribution of landslide damages in the study area

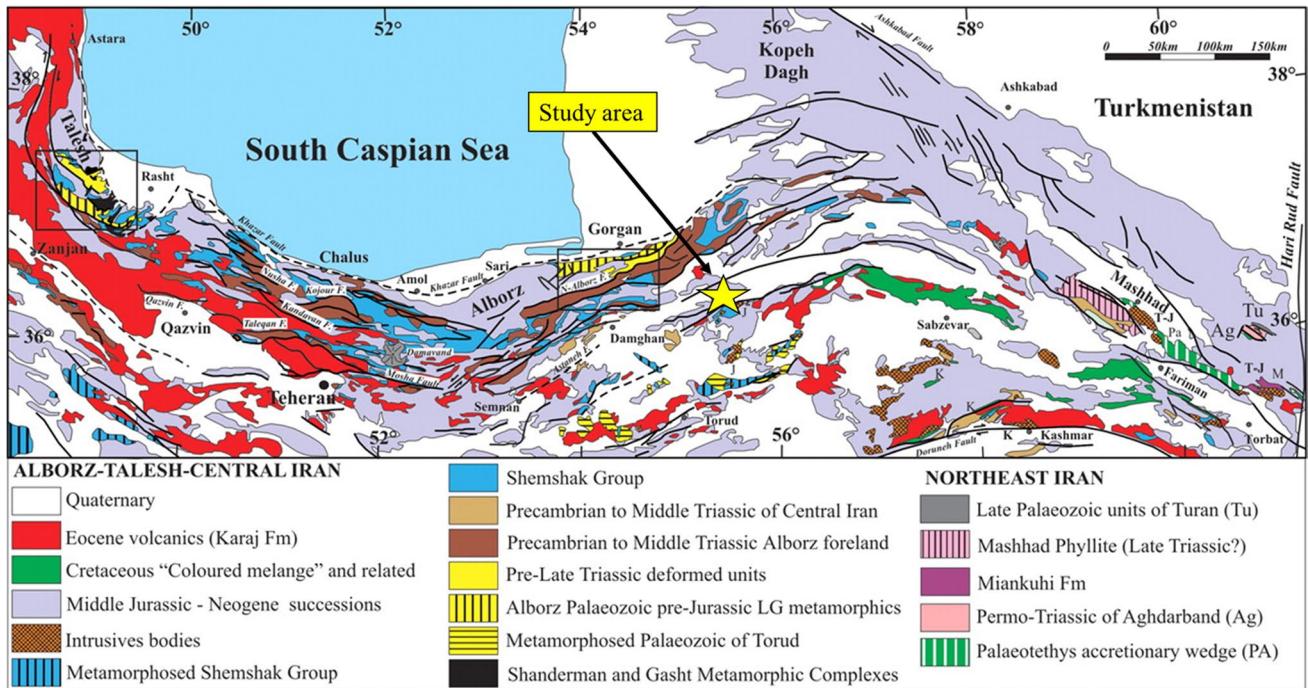**Fig. 6** Geotechnical and structural damages during the Kalpush landslide

Fig. 7 Geological map of the study area (after Zanchi et al. 2009)

Figure 6d indicates a road pavement that was destroyed during the landslide.

Geotechnical and geological properties

The geological map of the Kalpush landslide is shown in Fig. 7. Figure 7 demonstrates that the dam has been constructed on the sedimentary rocks of the limestone formed in the Jurassic period. The RQD values of the rocks (< 50) indicated that the rock mass quality is in terms of poor and very poor (IRHFS 2019). The rocks are highly weathered based on the field investigation and the correlation between weathering and RQD values (Ayalew et al. 2002). Moreover, the permeability of rocks has increased due to weathering. Accordingly, the grouting technic was used to decrease the permeability during the construction of the dam. The control test after grouting has shown that the degree of permeability decreased as an impervious layer (IRHFS 2019). Furthermore, the soft clay covered the slopes of the dam.

The geotechnical and geophysical data are not available in the sliding area. However, geotechnical borehole and geophysical down-hole data were provided near the landslide area. The location of the boreholes is shown in Fig. 8. As shown in this figure, the boreholes were carried out about 400 m far from the Kalpush landslide. Moreover, the variations of the shear wave velocity (V_s) were plotted versus depth in Fig. 8. The shear wave velocity was measured up to the depth of 12 m by a down-hole test. The
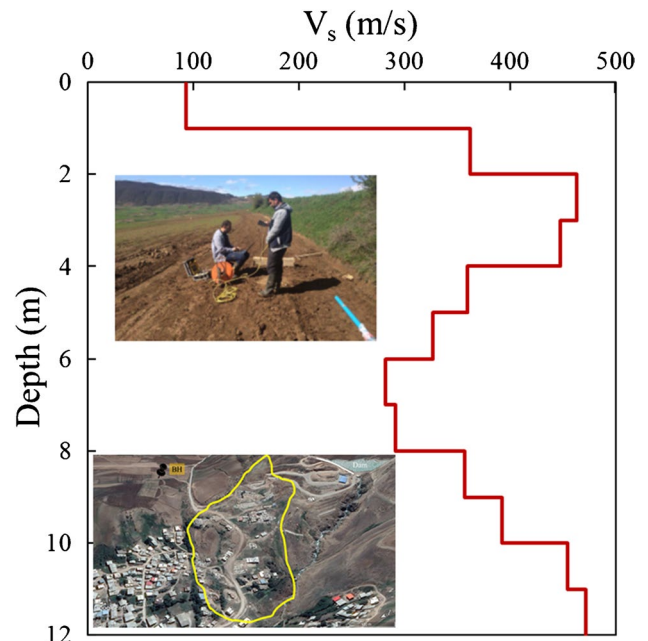

Fig. 8 Variations of the shear wave velocity

average value of V_s is around 359 m/s at depths of 0–12 m. The different geotechnical tests including the physical and mechanical tests were carried out on the soil samples. The results of the tests are summarized in Table 1. The grain size data shows the samples fall within the range of low plasticity of clay (CL).

Table 1 Geotechnical characteristics of the soil samples

Parameter	Standard	Value	
		Layer 1	Layer 2
LL (%)	ASTM D4318	35.5	-
PI (%)		14.7	-
γ_{wet} (kN/m^3)	ASTM D7263	19	20
γ_{sat} (kN/m^3)		20	21
G_s	ASTM D792	2.7	2.7
C' (kPa)	ASTM D2080	15	25
ϕ'°		25	31
K (m/s)	Correlation*	1×10^{-6}	1×10^{-7}
E (kPa)	Correlation	4000	10,000
ν	-	0.33	0.33
Thickness (m)	-	0–20	20–200

*Based on Hazen's (1911) correlation

It is noted that the consideration of three-dimensional particle geometries can provide a realistic estimation of soil properties (Zheng et al. 2021a, b).

The experimental results show that the surface layer of the soil is relatively weak at depths of 0–9 m and then the shear wave velocity increases at lower depths. As cited, the rocks of the site are highly weathered along with joints and cracks as a permeable layer. Accordingly, water seepage can play an important role in landslide occurrence when the dam reservoir is filled to maximum capacity. However, the permeability of the rock was decreased by the grouting method based on the geotechnical reports during the dam construction processes.

Rainfall data and landslide formation process

Figure 9 shows the distribution of rainfall in the Kalpush/village area. Figure 9a indicates that the intensity of rainfall has significantly increased from January to March when the maximum deformations have been observed. As seen in Fig. 9(a), abnormal intensive rainfall has occurred in this area for 3 months so that rainfall intensity is around 6 times the long-term average value. Moreover, Fig. 9b shows daily rainfall from 12 March to 10 April. Figure 9b demonstrates that the cumulative rainfall intensity is around 337.8 mm for a month which is 7.5 times the long-term average value. For example, 238.4 mm of rainfall occurred from 18 to 20 March. According to Guzzetti et al. (2008), the rainfall threshold for the initiation of a landslide can be estimated by Eq. (1) as follows:

$$I = 2.2D^{-0.44} \tag{1}$$

Moreover, Jia et al. (2020) employed the satellite-based rainfall data and global landslide catalog including landslide occurrence in Iran to develop global rainfall—global rainfall thresholds as follows:

$$I = 0.99D^{0.7} \tag{2}$$

where I is the rainfall intensity per mm/h and D is the rainfall duration per h or days in Eqs. (1)-(2).

Based on Eqs. (1) and (2), the rainfall threshold for landslide triggering is estimated around 52.8 and 23.76 mm/d, respectively while Fig. 9b shows that a 134.2 mm/d rainfall occurred on 19 March. Accordingly, there was a potential rainfall-induced landslide in this area.

The variations of the annual water discharge of the Hosein Abad and Ghooshe Degereman rivers are shown in Fig. 10 based on long-term average data. These two rivers are the main sources of water entering the Kalpush dam lake. Figure 10 shows that a large volume of water enters the dam by rivers from March to May. The maximum water discharge is around 1.6 Mm3 in March and the minimum water discharge is around 0.4 Mm3 in October. However, the data of the measured monthly reservoir water levels are not available. Accordingly, the water level of the dam changes during different months which can affect the slope stability of downstream. The groundwater flow and rainfall can simultaneously affect the stability of the downstream slope.

A conceptual model of the mechanism and formation process of the Kalpush landslide is plotted in Fig. 11. As shown in this figure, two important factors have caused the huge landslide: (1) the precipitation and heavy rainfall and snowfall infiltrations into CL, and (2) the groundwater flow (seepage) from the river and the dam into the weathering rock mass and the saturated downstream layer. The variations of these two factors can lead to large deformations (e.g., Sun et al. 2013; Liu et al. 2017; Jafarian and Lashgari 2017; Kalubowila et al. 2021). As shown in Fig. 11, the water flow is concentrated at the border of two soil layers because of different permeability coefficients. It can provide a potential slippage surface and lead to the CL movement on the underlying layer. Accordingly, a large-scale slide as a translational landslide has gradually occurred in the area. Moreover, the precipitation can intensify the slope sliding. This failure mechanism can be observed in different case histories in the world (e.g., Zygouri and Koukouvelas 2019; Guo et al. 2019; Li et al. 2019).

Numerical simulation

A series of numerical simulations were carried out to comprehend the failure mechanism of the slope using the evaluation of rainfall and seepage effects as discussed in Fig. 11.

Fig. 9 Characteristics of rainfall of the Kalpush area. **a** Monthly rainfall and **b** daily rainfall (after Entezam et al. 2019)

(a)

(b)
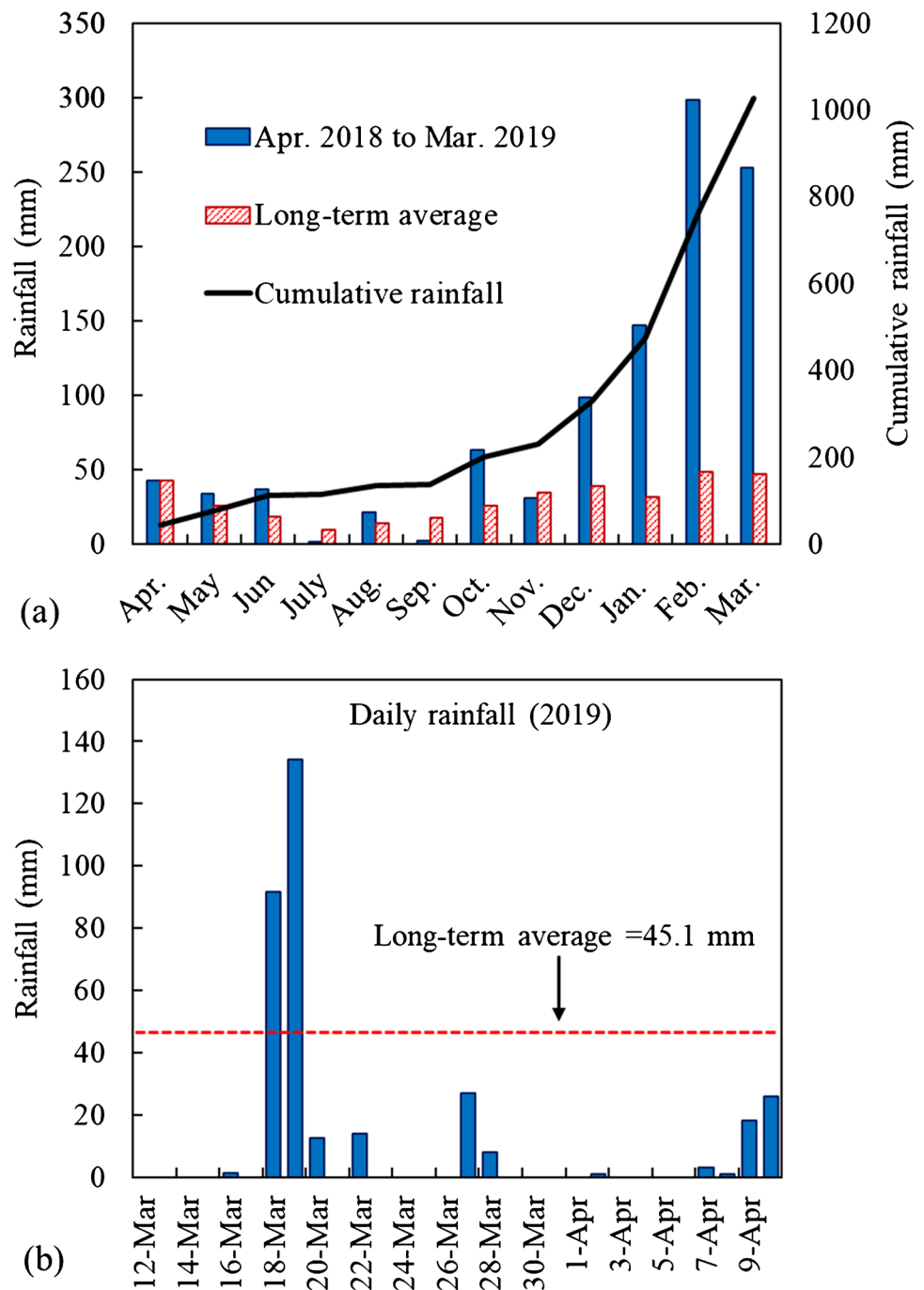
The behavior of soil layers was modeled by the Mohr–Coulomb model. The input parameters of the Mohr–Coulomb model were obtained from soil test results shown in Table 1. The initial stress within the soil body was generated using the PLAXIS 2D gravity loading. The standard fixities were applied as the mechanical boundary. The factors of safety (FS) were evaluated using the fully coupled flow-deformation analysis. The soil hydraulic and mechanical responses were calculated simultaneously in the fully coupled flow-deformation analysis. The mesh dimensions were selected using sensitivity analysis so that mesh density is considered higher in the sliding zone. The numerical analyses were carried out for three cross sections shown in Fig. 12.

Evaluation of the rainfall effect

The rainfall intensity as a daily average for 3 months from January to March was applied to the slope model. The values of the rainfall intensities are shown in Fig. 9. The maximum iteration number and tolerance limit were assumed 100 and
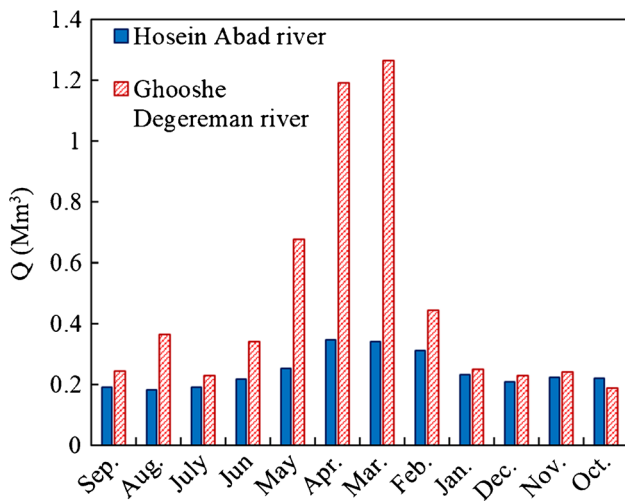
Fig. 10 Variation of the annual discharge of Hosein Abad and Ghooshe Degereman rivers (after Entezam et al. 2019)

0.01 for analyses, respectively. The factors of safety (FS) and sliding surfaces were shown before and after rainfall for three sections in Fig. 13(a-e). Figure 13 indicates that the mean value of FS is greater than 1.5 before rainfall. However, the mean value of FS decreases to less than 1.5 after rainfall. Moreover, the highest reduction of FS occurs in section b-b so that FS = 1 shows the sliding threshold. It is noted that FS < 1.2 was proposed by Naidu et al. (2018) for the rainfall threshold. Figure 13 demonstrates that rainfall led to a decrease in the factor of safety by around 1.48 times. Accordingly, landslide occurrence is inevitable in this area after rainfall. The potential slip surfaces shown in Fig. 13 demonstrate that the whole study area is prone to shallow sliding.

As shown in Figs. 5–6, the most damage was observed along section b-b where the lowest FS (= 1) has been obtained from numerical analysis. Accordingly, section b-b as a critical section was selected for the deformation numerical analysis. Figure 14 shows the sliding displacement of section b-b before and after rainfall. Figure 14a and b indicate that the maximum displacement of the slope is around 3.5 cm before rainfall while it has increased by 43 cm after rainfall. Accordingly, the structures located in this area experienced large deformations in near-collapse and collapse levels (> 5 mm) after rainfall as observed damages indicate.

Fig. 11 Conceptual model of the mechanism and formation process of the Kalpush landslide
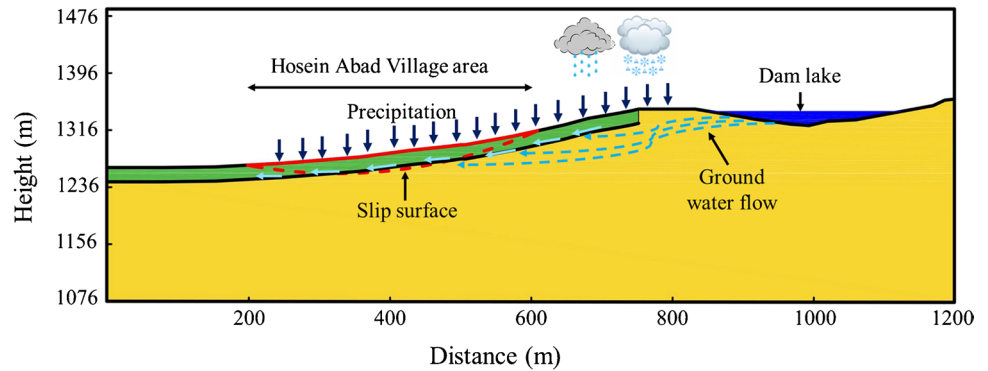

Fig. 12 Locations of the selected slope cross sections for numerical modeling
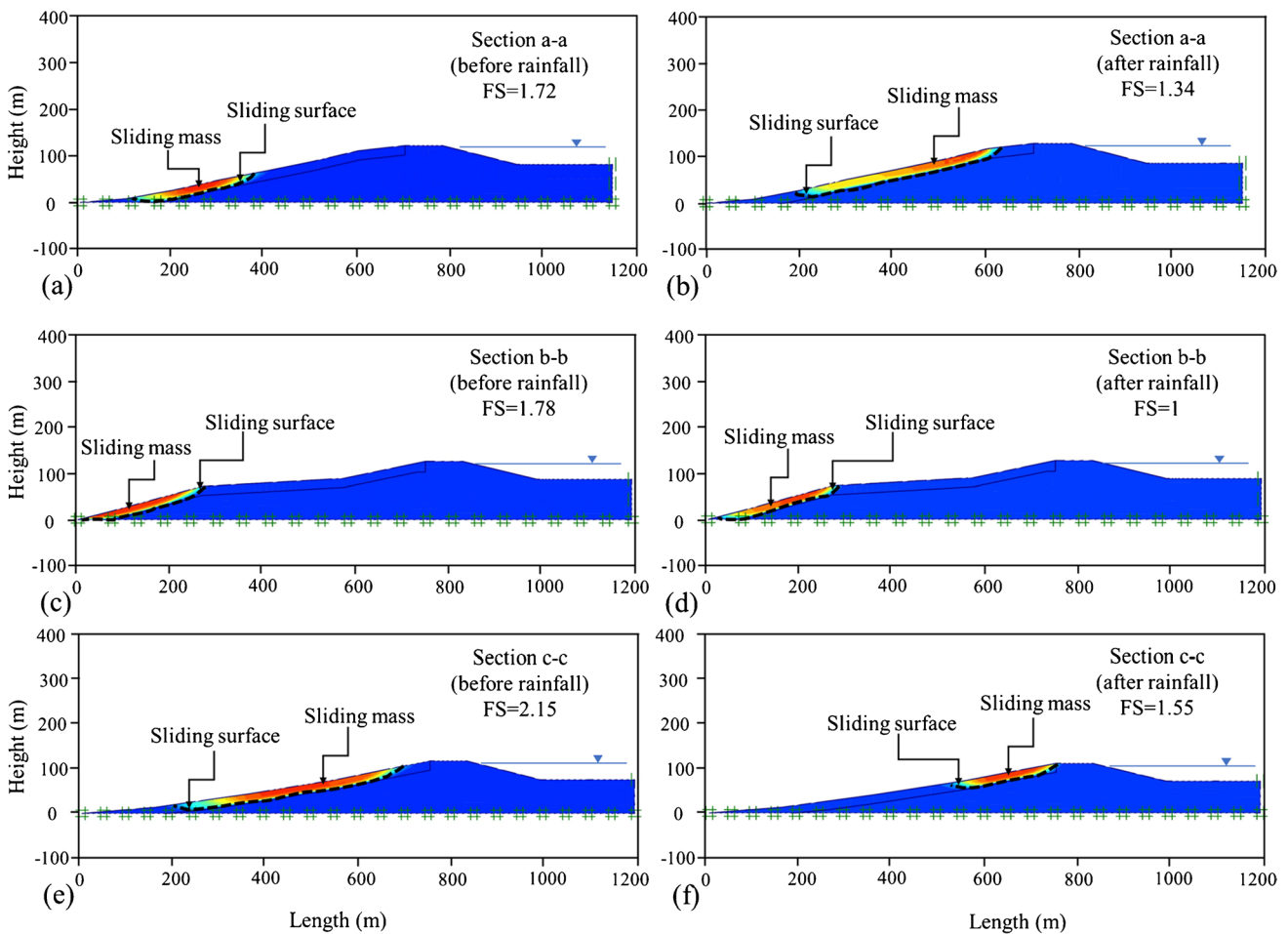
Fig. 13 Safety factor and the sliding surface of the selected sections before and after rainfall

Evaluation of the seepage effect

A number of the village residents reported that the building tracks and water accumulation in the basement were observed several months before rainfall. Accordingly, the groundwater flow was analyzed for evaluation of the seepage effect on slope instability. Figure 15 shows the vector of the flow path during seepage and before rainfall. Figure 15 illustrates that the concentration of flow vectors occurs at the border of two layers in the main body and toe of the slope. Accordingly, this flow path can cause the CL to slip on the bottom layer.

As shown in Fig. 9, the amount of water entering the dam changes during different months which can affect the water level of the dam. Accordingly, a series of numerical analyses were carried out to study the effect of water seepage on the downstream slope stability regardless of precipitation. However, the data of the measured monthly reservoir water levels are not available. The variations of the slope safety factor were plotted versus the variations of the water level in Fig. 16. As Fig. 16 shows, the factor of safety decreases from

1.88 to 1.78 when the water level increases. Accordingly, the variations of water level as an important factor can lead to an unstable condition for the downstream slope. However, the decreased safety factor is not less than the allowable safety factor (> 1.5).

Landslide mitigation strategies

Several methods are employed to mitigate soft soils and landslide hazards based on the ground improvement techniques including mechanical methods (e.g., shallow and deep-compaction techniques), hydraulic methods (e.g., dewatering systems), physical and chemical methods (e.g., grouting and modification by admixture methods), and soil reinforcement methods (e.g., soil nailing method). The selection of a ground modification technic depends on several factors such as failure triggering mechanism, soil properties, and construction cost. Alimohammadi et al. (2022) presented the advantages, limitations, proposes, and design considerations of the deep-compaction method that is useful

Fig. 14 Total displacement of slope. **a** Before rainfall and **b** after rainfall
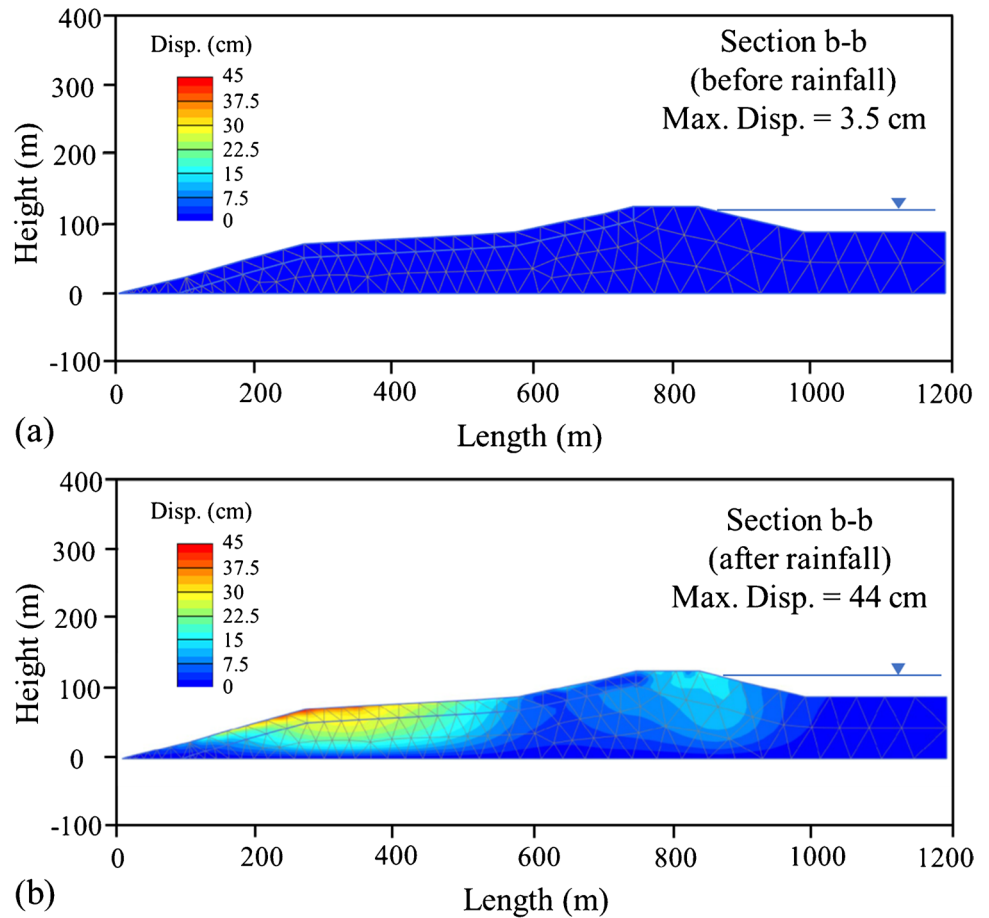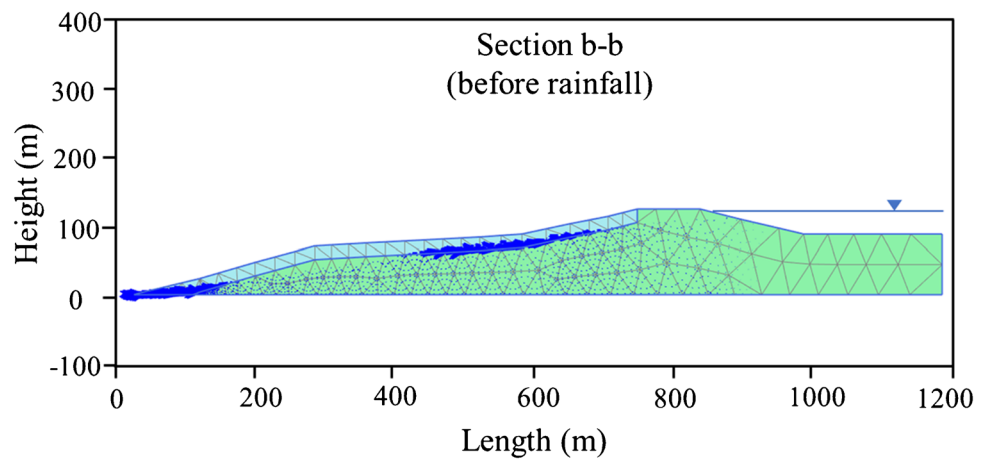

(a)

(b)

Fig. 15 The vectors of groundwater flow during seepage analysis

for geotechnical design engineers and design purposes. The geocells and piles as reinforcement strategies can appropriately reduce the stress level for soil improvement aims (e.g., Ardakani and Namaei 2021; Hashim and Muntohar 2006; Hegde and Sitharam 2015). However, the combination of vertical and lateral loadings can affect the performance of the piled raft foundations (Deb and Pal 2020; 2021).

In this paper, two landslide mitigation strategies have been investigated for the Kalpush landslide, including (1) the use of the deep soil mixing wall method (DSMW) and (2) the combination of DSMW and soil densification method. In the first technique, the number of nine DSMWs was considered at the different positions of the slope. The position of the DSMWs is shown in Fig. 17(a). The width of DSMWs is assumed 5 m and the distance of the
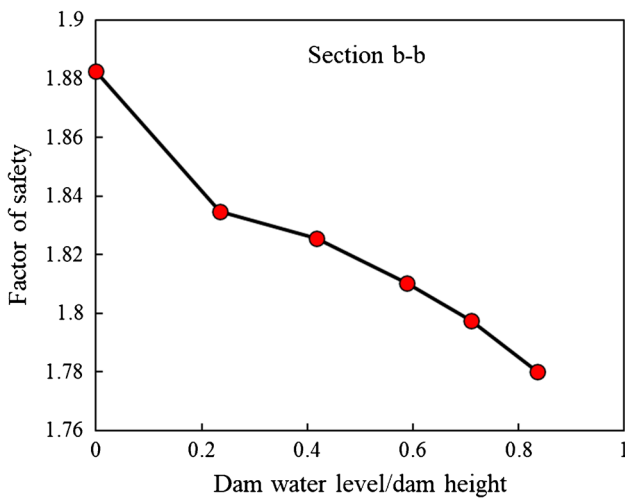
Fig. 16 Variations of safety factor versus the variations of dam water level

DSMWs was considered less in the critical sliding zone (see Fig. 14(b)). The mesh dimensions were refined for the analyses of mitigation strategies. According to Fan et al. (2018), the soil–cement mixture properties of walls are taken

as, unconfined compressive strength of 500 kPa, friction angle of 36°, cohesion of 160.8 kPa, and elastic modulus of 417,850.1 kPa. Figure 17b indicates that the maximum displacement of slope decreases from 44 to 25 cm when the DSMWs are employed for landslide hazard mitigation. Moreover, a comparison of Figs. 14(b) and 17(b) indicates that the depth of the sliding zone decreases after the use of the DSMW so that the sliding zone changes from a deep zone to a shallow zone.

Figure 17 shows that the failure zone changes to a shallow zone after the use of the DSMW. However, the displacement of the slope is relatively large in the shallow zone. Previous studies (e.g., Jafarian et al. 2014; Hegde and Sitharam 2015; Zheng et al. 2021a, b; Alimohammadi et al. 2022) showed that the use of soil densification methods (e.g., deep compaction, vibroflotation, soil-fiber mixtures, geocell reinforcement) can increase the shear strength and the stability of slopes. Accordingly, the soil densification method was considered to compact the soil layer to mitigate landslide hazards besides the DSMW technique. The compacted soil layers are shown in Fig. 18(a). Based on Ameratunga et al. (2016), the properties of the compacted soil layer are taken as, friction angle of 32°, cohesion of 20 kPa, and elastic modulus of 10,000 kPa. The variations

Fig. 17 Performance of DSMW technique for landslide mitigation. **a** Location of DSMWs and **b** total displacement of slope
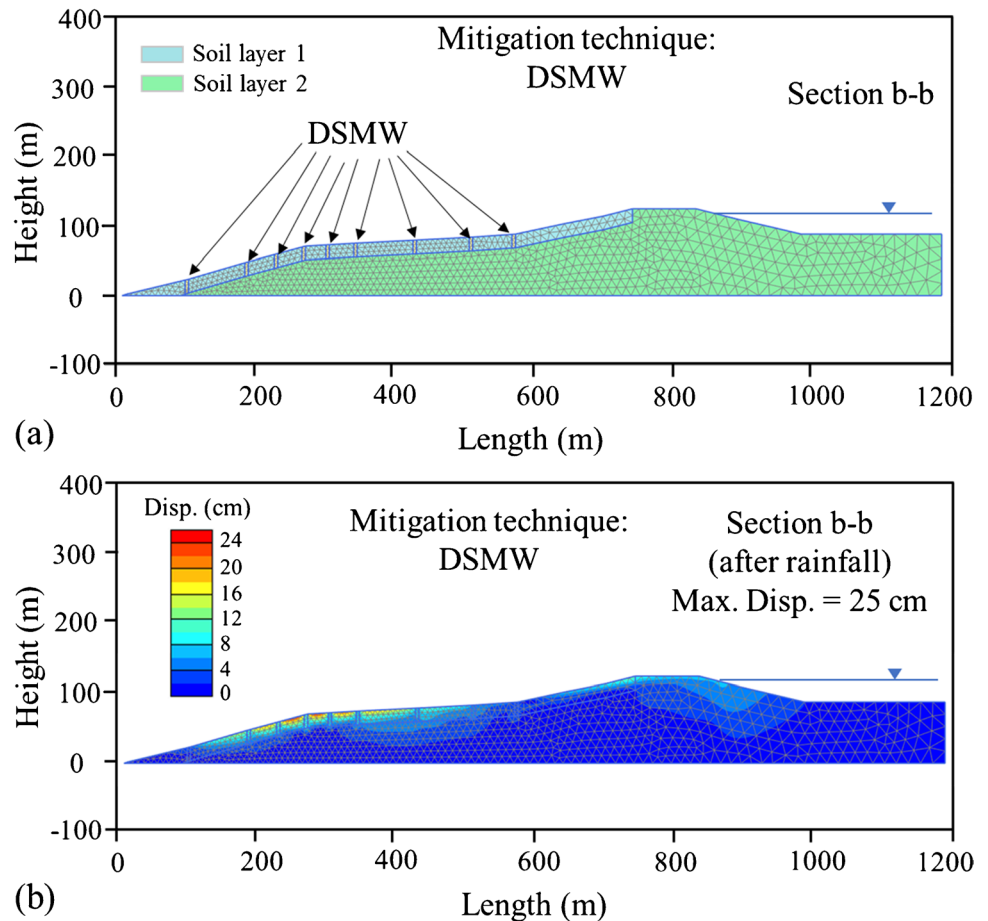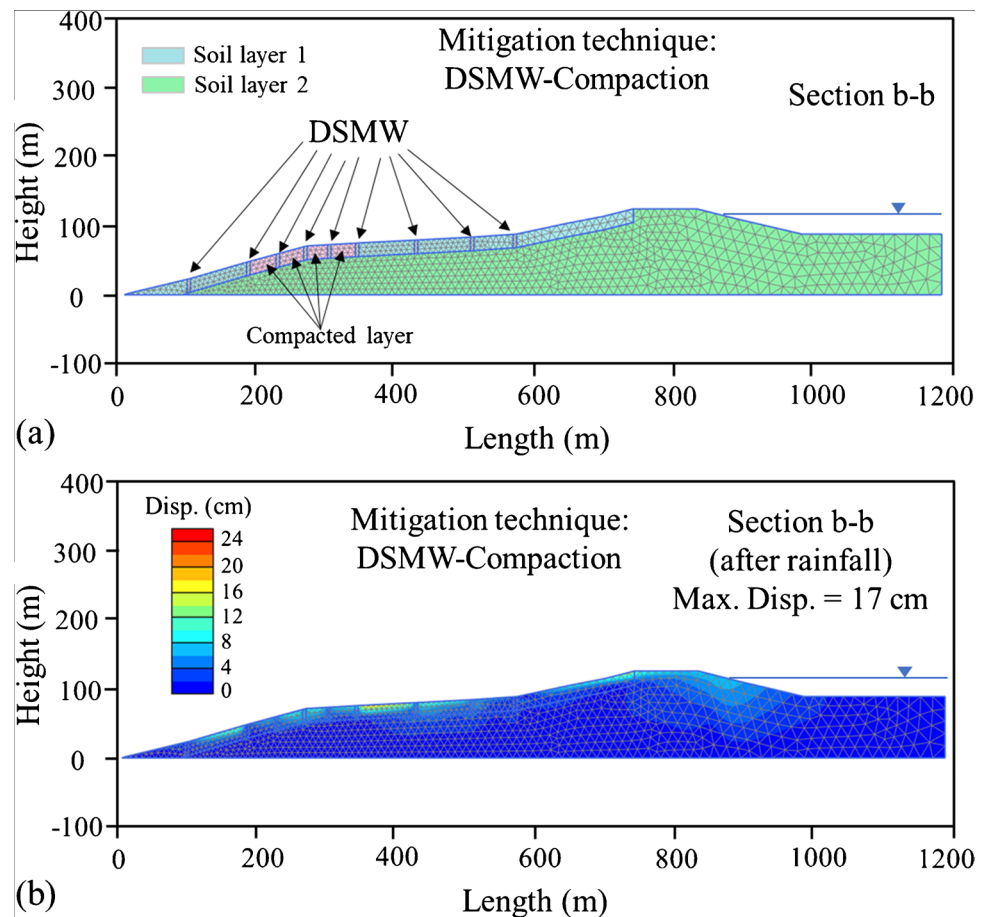
Fig. 18 Performance of DSMW-compaction technique for landslide mitigation. **a** Positions of DSMWs and compacted soil layer and **b** total displacement of slope

of displacements are shown in Fig. 18(b) after the use of a combined landslide mitigation strategy. Figure 18b demonstrates that the use of a combination method can decrease the displacement of the slope by around 41% compared with the use of only the DSMW technique. Moreover, the displacement decreases from 25 to 8 cm in the critical sliding zone shown in Fig. 14(b). It is noted that the results of this study are based on assumptions of numerical modeling (e.g., used soil model, the uncertainty of soil, and rainfall parameters) and the consideration of these assumptions can develop rainfall-induced landslides in the future.

Conclusions

The current paper presented the preliminary results of field surveys and experimental investigation of a massive translational landslide triggered by the rainfall, snowfall, and seepage of the dam in Kalpush Village, Meyami County, Semnan Province, Iran. The landslide significantly affected buildings located on the sliding mass and 250 houses experienced the collapse and near-collapse levels.

The site investigations indicate that the landslide potential is high in the study region. Two important factors have caused the destructive landslide in this area: (1) seepage flow from the upstream toward the downstream of the dam and (2) heavy rainfall for 3 months. A large volume of water entered the dam through the Hosein Abad and Ghooshe Degereman rivers from March to May. Accordingly, the water level of the dam changed during these months which can affect the slope stability of downstream. The rainfall data during January and March indicated that the cumulative rainfall intensity is 7.5 times the long-term value. The rainfall intensity is around 2.5 times the rainfall threshold for landslide triggering.

The numerical simulations for three sections of the sliding area indicated that the factor of safety of slope averagely decreases around 1.48 times after rainfall occurrence. The FS of the middle of the sliding mass as the critical section decreased from 1.78 to 1 after rainfall. The slope displacement increased around 12.3 times after rainfall which caused the structures to experience collapse. The seepage analysis demonstrated that the concentration of groundwater flow occurs at the border of CL and the bottom layer. Accordingly, this flow path is led to the CL slipping on the bottom layer. The seepage analysis demonstrated that the concentration of groundwater flow occurs at the border of CL and the bottom layer. Accordingly,

this flow path is led to the CL slipping on the bottom layer. Moreover, the variations of the dam water level can decrease the safety factor from 1.88 to 1.78.

The comparison of improving slope stability techniques showed that a combination technique can reduce the displacement by around 41% compared with the use of only one ground improvement method. Moreover, the displacement decreases from around 25 to 8 cm in the critical sliding zone. The results of the study can provide a perspective on the climate change impacts in Iran for future geosystem designs, geohazard prediction, and the selection of rainfall-induced landslide mitigation strategies.

Declarations

Conflict of interest The authors declare no competing interests.

References

Zhao N, Hu B, Yi Q, Yao W, Ma C (2017) The coupling effect of rainfall and reservoir water level decline on the Baijiabao landslide in the Three Gorges Reservoir Area, China. Geofluids 2017:1–12. https://doi.org/10.1155/2017/3724867

Zheng G, Alimohammadi H, Zheng J, Schaefer VR (2021a) Effectiveness of geosynthetics in the construction of roadways: a full-scale field studies review. IFCEE 2021:223–232

Zheng J, He H, Alimohammadi H (2021b) Three-dimensional Wadell roundness for particle angularity characterization of granular soils. Acta Geotech 16(1):133–149

Zygouri V, Koukouvelas IK (2019) Landslides and natural dams in the Krathis River, north Peloponnese, Greece. Bull Eng Geol Env 78(1):207–222

Askarinejad A, Laue J, Zweidler A, Iten M, Bleiker E, Buschor H, Springman SM (2012) Physical modelling of rainfall induced landslides undercontrolled climatic conditions. In Proceedings of the Conference Eurofuge 2012, Delft, Netherlands, Published on CD only

Ayalew D, Barbey P, Marty B, Reisberg L, Yirgu G, Pik R (2002) Source, genesis, and timing of giant ignimbrite deposits associated with Ethiopian continental flood basalts. Geochim Cosmochim Acta 66(8):1429–1448

Alimohammadi H, Amirmojahedi M, Tahat JN (2022) A case history of application of deep compaction method with comparison to different ground improvement techniques. Transp Infrastruct Geotechnol 1–26. https://doi.org/10.1007/s40515-022-00229-3

Alimohammadlou Y, Najafi A, Gokceoglu C (2014) Estimation of rainfall-induced landslides using ANN and fuzzy clustering methods: a case study in Saeen Slope, Azerbaijan province. Iran Catena 120:149–162

Ameratunga J, Sivakugan N, Das BM (2016) Correlations of soil and rock properties in geotechnical engineering. Springer New Delhi. https://doi.org/10.1007/978-81-322-2629-1

Ardakani A, Namaei A (2021) Geocell reinforced slope behavior under seismic loading using calibrated hypoplastic soil constitutive model. J Rehabil Civ Eng 9(4):77–92. https://doi.org/10.22075/jrce.2021.21425.1446

Building and Housing Research Center (BHRC) (2014) Iranian code of practice for seismic resistant design of buildings (standard no. 2800). 4rd Edition, Building and Housing Research Center, Tehran, Iran

Caine N (1980) The rainfall intensity-duration control of shallow landslides and debris flows. Geogr Ann Ser B 62(1–2):23–27

Chien-Yuan C, Tien-Chien C, Fan-Chieh Y, Sheng-Chi L (2005) Analysis of time-varying rainfall infiltration induced landslide. Environ Geol 48(4):466–479

Dahal RK, Hasegawa S (2008) Representative rainfall thresholds for landslides in the Nepal Himalaya. Geomorphology 100(3–4):429–443

Dang K, Sassa K, Konagai K, Karunawardena A, Bandara RMS, Hirota K, ..., Ha ND (2019) Recent rainfall-induced rapid and long-traveling landslide on 17 May 2016 in Aranayaka, Kagelle District, Sri Lanka. Landslides 16(1):155–164

Deb P, Pal SK (2020) Nonlinear analysis of lateral load sharing response of piled raft subjected to combined VL loading. Mar Georesour Geotechnol 39(8):994–1014

Deb P, Pal SK (2021) Influence of combined vertical and lateral loading on lateral response of piled raft foundation. In Proceedings of the Indian Geotechnical Conference 2019, Surat, India, 19–21 December 2021; pp. 395–406

Di B, Stamatopoulos CA, Stamatopoulos AC, Liu E, Balla L (2021) Proposal, application and partial validation of a simplified expression evaluating the stability of sandy slopes under rainfall conditions. Geomorphology 395:107966

Entezam I, Rezari A, Vakilzade Y, Mohammadi Y, Babazade N (2019) Evaluation and analysis of the Hosein Abad Kalpush landslide. Report TR040, National Geoscience Database of Iran

Fan J, Wang D, Qian D (2018) Soil-cement mixture properties and design considerations for reinforced excavation. J Rock Mech Geotech Eng 10(4):791–797

Guo C, Zhang Y, Li X, Ren S, Yang Z, Wu R, Jin J (2019) Reactivation of giant Jiangdingya ancient landslide in Zhouqu County, Gansu Province, China. Landslides 1–12

Guzzetti F, Peruccacci S, Rossi M, Stark CP (2008) The rainfall intensity–duration control of shallow landslides and debris flows: an update. Landslides 5(1):3–17

Hashim R, Muntohar AS (2006) Swelling rate of expansive clay soils. In: Al-Rawas AA, Goosen ZFA (eds) Expansive soils: recent advances in characterization and treatment. Taylor & Francis, Abingdon, UK, pp 139–148

Hazen A (1911) Discussion of dams on sand foundations. Koenig AC ed., Trans Am Soc Civ Eng 73(3):199–203

Hegde AM, Sitharam TG (2015) Three-dimensional numerical analysis of geocell-reinforced soft clay beds by considering the actual geometry of geocell pockets. Can Geotech J 52(9):1396–1407

Highland L, Bobrowsky PT (2008) The landslide handbook—a guide to understanding landslides. U.S. Geological Survey Circular, Reston, Virginia, p. 129

IPCC Climate Change (2013) The physical science basis. Contribution of working group I to the fifth assessment report of the intergovernmental panel on climate change (IPCC), Cambridge University Press, UK and USA, 2013

Islamic Revolution Housing Foundation of Semnan (2019) Final geotechnical report of the suggested site for the development of the Kalpush village. Islamic Revolution Housing Foundation of Semnan (IRHFS), Semnan, Iran

Jafarian Y, Lashgari A (2017b) Seismic sliding analysis of sandy slopes subjected to pore-water pressure buildup. Int J Geomech 17(11):04017106

Jafarian Y, Miraei M, Lashgari A, Shakeri P (2014) Probabilistic evaluation of dynamic response of caisson quay walls in soil improved by fiber: a numerical study. In Numerical methods in geotechnical engineering, edited by Hicks M, Brinkgreve R, and Rohe A, 909–914. Leiden, Netherlands: CRC Press/A. A. Balkema

Jafarian Y, Lashgari A (2017a) Closure to "Simplified procedure for coupled seismic sliding movement of slopes using displacement-based critical acceleration" by Yaser Jafarian and Ali Lashgari. Int J Geomech 17(9). https://doi.org/10.1061/(ASCE)GM.1943-5622.0000971

Javdanian H, Pradhan B (2019) Assessment of earthquake-induced slope deformation of earth dams using soft computing techniques. Landslides 16(1):91–103

Jafarian Y, Lashgari A, Haddad A (2019) Predictive model and probabilistic assessment of sliding displacement for regional scale seismic landslide hazard estimation in Iran. Bull Seismol Soc Am 109(5):1581–1593. https://doi.org/10.1785/0120190004

Javdanian H, Zarei M, Shams G (2022) Estimating seismic slope displacements of embankment dams using statistical analysis and numerical modeling. Model Earth Syst Enviro 9:389–396. https://doi.org/10.1007/s40808-022-01505-4

Jia G, Tang Q, Xu X (2020) Evaluating the performances of satellite-based rainfall data for global rainfall-induced landslide warnings. Landslides 17(2):283–299

Kalubowila P, Lokupitiya E, Halwatura D, Jayathissa G (2021) Threshold rainfall ranges for landslide occurrence in Matara district of Sri Lanka and findings on community emergency preparedness. Int J Dis Risk Reduct 52:101944

Kristo C, Rahardjo H, Satyanaga A (2017) Effect of variations in rainfall intensity on slope stability in Singapore. Int Soil Water Conserv Res 5(4):258–264

Lashgari A, Jafarian Y, Haddad A (2018) Predictive model for seismic sliding displacement of slopes based on a coupled stick-slip-rotation approach. Eng Geol 244:25–40. https://doi.org/10.1016/j.enggeo.2018.07.017

Lashgari A, Jafarian Y, Haddad A (2021) Predictive model for seismic sliding displacement of slopes subjected to pulse-like motions. Bull Eng Geol Env 80(8):6563–6582

Lashgari A, Jafarian Y, Haddad A (2020) A coupled stick-slip-rotation model for earthquake-induced sliding displacement of slopes in Iran. Soil Dyn Earthq Eng 135:106199

Li C, Yao D, Wang Z, Liu C, Wuliji N, Yang L, ..., Amini F (2016) Model test on rainfall-induced loess–mudstone interfacial landslides in Qingshuihe, China. Environ Earth Sci 75(9):1–18

Li D, Yan L, Wu L, Yin K, Leo C (2019) The Hejiapingzi landslide in Weining County, Guizhou Province, Southwest China: a recent slow-moving landslide triggered by reservoir drawdown. Landslides 16(7):1353–1365

Liu J, Yang C, Gan J, Liu Y, Wei L, Xie Q (2017) Stability analysis of road embankment slope subjected to rainfall considering runoff-unsaturated seepage and unsaturated fluid–solid coupling. Int J Civ Eng 15(6):865–876

Loo YY, Billa L, Singh A (2015) Effect of climate change on seasonal monsoon in Asia and its impact on the variability of monsoon rainfall in Southeast Asia. Geosci Front 6(6):817–823

Naidu S, Sajinkumar KS, Oommen T, Anuja VJ, Samuel RA, Muraleedharan C (2018) Early warning system for shallow landslides using rainfall threshold and slope stability analysis. Geosci Front 9(6):1871–1882

Palmisano F, Vitone C, Cotecchia F (2018) Assessment of landslide damage to buildings at the urban scale. J Perform Constr Facil 32(4):04018055

Paswan AP, Shrivastava AK (2022) Modelling of rainfall-induced landslide: a threshold-based approach. Arab J Geosci 15(8):1–19

Rivera-Hernandez XA, Ellithy G, Vahedifard F (2019) Integrating field monitoring and numerical modeling to 3 evaluate performance of a levee under 4 climatic and tidal variations. J Geotech Geoenviron Eng 145(10):1

Sun H, Zhong J, Zhao Y, Shen S, Shang Y (2013) The influence of localized slumping on groundwater seepage and slope stability. J Earth Sci 24(1):104–110

USGCRP (US Global Change Research Program) (2009) Global climate change impacts in the United States. Cambridge University Press, Washington, DC

Vaghefi SA, Keykhai M, Jahanbakhshi F, Sheikholeslami J, Ahmadi A, Yang H, Abbaspour KC (2019) The future of extreme climate in Iran. Sci Rep 9(1):1–11

Vahedifard F, Tehrani FS, Galavi V, Ragno E, AghaKouchak A (2017) Resilience of MSE walls with marginal backfill under a changing climate: quantitative assessment for extreme precipitation events. J Geotech Geoenviron Eng 143(9):04017056.

Vasseghi A, Haghshenas E, Soroushian A, Rakhshandeh M (2021) Failure analysis of a natural gas pipeline subjected to landslide. Eng Fail Anal 119:105009

Zanchi A, Zanchetta S, Berra F, Mattei M, Garzanti E, Molyneux S, ..., Sabouri J (2009) The Eo-Cimmerian (Late? Triassic) orogeny in North Iran. Geological Society, London, Special Publications 312(1):31–55

Zhang A, Zhang P, Dai Z, Huang B, Zhang C, Wang L, Jiang X (2022) Failure mechanism of the Simiqiao landslide under rainfall and slope cutting. Arab J Geosci 15(17):1–16